Modulation of Gap Junction Transcript and Protein Expression during Pregnancy in the Rat

Boris Risek, Sarah Guthrie, Nalin Kumar, and Norton B. Gilula

Department of Molecular Biology, Research Institute of Scripps Clinic, La Jolla, California 92037

Abstract. The expression of three different gap junction transcripts, α_1 (Cx_{43}), β_1 (Cx_{32}), and β_2 (Cx_{26}) was examined in several organs during pregnancy in the rat. In all of the organs that were examined—uterus, ovary, heart, and liver—there was a strong correlation between levels of gap junction mRNA and gap junction antigens that were detected at different stages of pregnancy. A striking change in α_1 transcript levels (a 5.5-fold increase) was detected in the uterine myometrium on the day before parturition. This elevation of the α_1 transcript is thought to be associated with the formation of gap junctions that are required for synchronizing the contractility of the myometrial cells during parturition. 2 d before parturition, there was a detectable elevation of β_2 transcripts and protein in the endometrial epithelium, which was then followed by a dramatic decrease in β_2 gap junctional protein on the day before parturition. There was also a substantial elevation of α_1 transcripts (a 6.7-fold increase) in the stromal regions of the ovary on the day before parturition that was identical to the temporal pattern of α_1 expression in the myometrium. In all three instances—the α_1 transcripts in the myometrium, β_2 transcripts in the endometrium, and α_1 transcripts in the ovary—the transcript modulation appeared to be cell specific, because the changes in transcript levels of these three gene products occurred independently of the poly(A)+RNA concentrations at the same pregnancy stages in the respective organs. There were no specific changes detected in gap junction transcript levels in the heart and liver during pregnancy. These observations indicate that a cell-specific modulation of gap junction expression occurs in two regions of the uterus and the ovary during pregnancy. Further, it appears that the same gap junction gene in different organs, such as the α_1 gene in the uterine myometrium and the heart, can be differentially regulated.

It is now well established that cell-to-cell communication in various tissues is mediated by specialized membrane regions known as gap junctions (Gilula et al., 1972; Loewenstein, 1981). Recent molecular characterizations have provided direct evidence for a family of related gap junction (GJ)[1] proteins that form intercellular channels. This includes the identification of cDNA clones coding for three different GJ proteins with deduced molecular masses of 32 kD from mammalian liver (Paul, 1986; Kumar and Gilula, 1986), 43 kD from mammalian heart (Beyer et al., 1987), and a 26-kD protein from mammalian liver (Nicholson and Zhang, 1988). A fourth candidate is a 70-kD junction protein component of the lens fiber junctions that has an amino terminus that is homologous to those of the liver and heart GJ proteins (Kistler et al., 1988; Beyer et al., 1989). Because all of these coding sequences have a conserved region of ~200 amino-terminal amino acid residues containing four putative transmembrane stretches with the amino- and carboxy-terminal residues likely to be located on the cytoplasmic side of the junction membrane, it has been possible to deduce a generalized structure for junctional membrane protein topology (Zimmer et al., 1987; Beyer et al., 1987; Milks et al., 1988; Goodenough et al., 1988; Nicholson and Zhang, 1988; Hertzberg et al., 1988; Yancey et al., 1989).

It has been known for some time that there are significant changes in GJ populations in various female reproductive organs during hormone-dependent events. For example, the mammalian preovulatory ovarian follicle contains a large population of GJs that connect granulosa cells to each other, as well as to the oocyte itself (Gilula et al., 1978; Larsen et al., 1981). The ovarian follicle undergoes dramatic changes in structure and activity during the menstrual cycle and pregnancy. An apparent downregulation of GJs has been reported during early and late preovulatory periods for the follicular cells and the cumulus-oophorus in response to an ovulatory stimulus (Larsen et al., 1981; Larsen et al., 1986), indicating that GJ structures can be regulated differentially within the same follicular unit.

Address correspondence to Dr. Norton B. Gilula, Department of Molecular Biology, Research Institute of Scripps Clinic, 10666 N. Torrey Pines Road, La Jolla, CA 92037.

1. *Abbreviations used in this paper*: GJ, gap junction; KLH, keyhole limpet hemocyanin.

GJs have been also documented to provide low-resistance pathways for electrical coupling between neighboring cells in several smooth muscle cell systems (for review see Daniel, 1987). This includes the uterine myometrium, which has been shown to dramatically increase its GJ content at parturition (term) (Garfield et al., 1977, 1978, 1982; Dahl and Berger, 1978; Saito et al., 1985; Ikeda et al., 1987) or after estrogen treatment of immature animals (Burghardt et al., 1984; Garfield et al., 1978). In addition to these morphological observations, a GJ transcript has been detected in term uterus (Beyer et al., 1987) and a major 43-kD protein has been detected in uterine samples using peptide antibodies prepared to a region of the rat heart GJ protein (Dupont et al, 1988; Beyer et al., 1989).

The present system that has been used to distinguish the different GJ gene products is based principally on the molecular weights of the deduced protein products (Beyer et al., 1987). Unfortunately, this approach has limitations because protein products of many different sizes have been reported (Table I), and similar genes in different organisms can produce protein products of slightly different sizes; i.e., the mammalian liver gene product is 32 kD (Paul, 1986; Kumar and Gilula, 1986), whereas the *Xenopus* liver gene product is 30 kD (Gimlich et al., 1988). Consequently, we have applied a Greek nomenclature that emphasizes genetic origin and sequence similarities (both nucleotide and amino acid) rather than protein product size. For this purpose, the gene for the 43-kD protein from the heart (Beyer et al., 1987) has been designated as the α_1 GJ gene, because the sequence for this protein is significantly different from those for the 32- and 26-kD proteins from the liver (Paul, 1986; Kumar and Gilula, 1986; Nicholson and Zhang, 1988). The sequences for the other two proteins are quite similar, and therefore have been designated as members of the β class of GJ genes: the 32-kD gene is referred to as the β_1 gene and the 26-kD gene is referred to as the β_2 gene (see Table I).

In this study we have examined the expression of three different GJ transcripts (α_1, β_1, β_2) and their related protein products in various tissues during different stages of pregnancy to determine if there is a modulation of GJ expression in response to hormonal stimuli during pregnancy.

Materials and Methods

I. Animals and Tissue Collection

Timed pregnant Wistar rats (220–250 g body weight), with a gestational period of 22 d, were obtained from Simonsen Laboratories (Gilroy, CA). Day 0 of pregnancy was defined by the presence of a uterine plug. The animals were maintained individually under a 12-h light/dark cycle with water and laboratory chow (Ralston-Purina Corp., St. Louis, MO) ad lib. and then decapitated at the following stages of pregnancy: day 18 (d-4), 20 (d-2), 21 (d-1), 22 (d0), 23 (d+1), 24 (d+2), and 26 (d+4). The day designations are relative to the day of parturition, which is defined as d0. At d0, tissues were taken between 3 and 6 h after parturition. The tissues were immediately removed and processed for indirect immunofluorescence or frozen in liquid nitrogen for RNA isolation. For RNA isolations from endometrial and myometrial samples, pre- and postpartum uteri were freed from placental and fetal material, and then separated into endometrium and myometrium by removing the endometrial layer with a scalpel. Subsequently, implantation sites were removed from myometrium. RNA from nonpregnant animals was extracted from whole uterus, because it was not possible to separate the endometrium from the myometrium in those specimens. RNA was routinely extracted from four animals at each time point.

Table I. Gap Junction Genes and Related Products

Gene	mRNA size	Deduced protein product size	Reported protein product sizes (Cx)	Reference*
	kb	*kD*	*kD*	
α_1	3.6	43	44–47, 43, 30, 28	Beyer et al., 1987
β_1	1.6	32	32, 28, 27, 26, 17, 10	Paul, 1986; Kumar and Gilula, 1986
β_2	2.8	26	26, 22, 21	Nicholson and Zhang, 1988

* Denotes reference to deduced protein product sizes.

II. Immunoblot Analysis and Immunohistochemistry

Affinity-purified antibodies prepared against synthetic peptides corresponding to a postulated cytoplasmic domain of the human β_1 liver (Milks et al., 1988), the mouse β_2 liver (Nishi, M., N. Kumar, and N. B. Gilula, manuscript in preparation), and rat α_1 heart GJ protein (Beyer et al., 1987) were used for the immunohistochemistry. This region of protein sequence has been designated the J region (Milks et al., 1988). The J epitope lies in a similar cytoplasmic surface location for these three proteins (α_1, β_1, β_2) according to current models of GJ topology (Zimmer et al., 1987; Beyer et al., 1987; Milks et al., 1988; Nicholson and Zhang, 1988), but is completely divergent in sequence for the α and β GJ proteins. The amino acid sequence for the J region in the α_1 protein extends from residues 131 to 142, from residues 111 to 125 for the β_1 protein, and from residues 112 to 125 for the β_2 protein (KNEFKDIEEIKTQK). These three peptide antibodies are designated in this study as α_1J, β_1J, and β_2J, respectively. Another peptide antibody that was prepared to a portion of the carboxy-terminal domain of the β_1 protein sequence has also been used in this study. This domain extends from residues 262 to 280 and has been designated as region S (Milks et al., 1988), and the antibody is identified as β_1S. All antibodies were prepared and characterized as described previously (Milks et al., 1988). The β_1J, β_2J, and α_1J antibodies were affinity-purified using corresponding synthetic peptide matrices. The β_1S antibody was affinity-purified using the purified native β_1 GJ protein.

β_1J and α_1J peptide antibodies were analyzed for reactivity and specificity by immunoblots against purified GJ protein isolated from rat liver or rat heart, respectively. Rat liver GJs were isolated using the alkali extraction procedure of Hertzberg (1984) as modified by Zimmer et al. (1987). Purified GJs isolated from rat heart according to the procedure of Manjunath and Page (1986) were kindly provided by Dr. Mark Yeager (Research Institute of Scripps Clinic, La Jolla, CA). β_2J peptide antibodies were characterized by immunoblot analysis of NaOH-insoluble homogenates prepared from nonpregnant liver and d-2 endometria. Tissues were alkali extracted (Hertzberg, 1984) and applied for analysis without further purification after protein determination (Lowry et al., 1951). SDS-PAGE and immunoblots were performed essentially as described by Milks et al. (1988), using the procedures of Laemmli (1970) and Towbin et al. (1979).

For indirect immunohistochemistry, small pieces of rapidly frozen fresh tissue were sectioned on a cryostat (Minotome; International Equipment Co., Boston, MA). Sections (from 3 to 5 μm) were collected on gelatinized slides and incubated with 3% BSA, 3% normal goat serum (Vector Laboratories, Burlingame, CA) in PBS (10 mM Na phosphate, pH 7.5, 0.9% NaCl) for 1 h at room temperature to reduce nonspecific binding. Incubation with peptide antibodies or preimmune rabbit IgG (5–10 μg/ml in 3% normal goat serum in PBS) was performed overnight at 4°C, followed by washing in PBS (three times for 15 min each). FITC-conjugated Fab' 2 goat anti-rabbit IgG (Cappel Laboratories, West Chester, PA) diluted 1:100 in PBS was then added and incubated at room temperature for 1 h. After incubation with the secondary antibody, the slides were washed (three times for 15 min each) in PBS and mounted in PBS containing 0.1% *N, N, N', N'*-tetramethyl-*p*-phenylenediamine, 90% glycerol. Immunolabeling was analyzed using a Zeiss Axiophot microscope with epifluorescence. All photographs were taken with Kodak T-MAX 400 black-and-white film (Eastman Kodak Co., Rochester, NY).

III. Extraction of Nucleic Acids and Normalization of poly(A)+ RNA

Total RNA was isolated by pulverization and homogenization of quick fro-

zen tissues in guanidine isothiocyanate (Chirgwin et al., 1979) followed by removal of DNA by overnight precipitation in 2 M LiCl (Palmiter, 1973). RNA was quantified by absorbance at 260 nm, and normalized for poly (A)+ RNA content by oligo(dT) hybridization as described by Harley (1987). In brief, total RNA was denatured in 6× SSC (1× SSC contains 0.15 M NaCl, 0.015 M Na citrate, pH 7.0) and 7.4% formaldehyde for 15 min at 65°C, and then applied to a nitrocellulose membrane (1 μg/100 μl) using a Minifold apparatus (Schleicher & Schuell, Keene, NH). A poly(A)+ standard (Pharmacia LKB Biotechnology, Inc., Pleasant Hill, CA) was quantified by absorbance at 260 nm and spotted on nitrocellulose as described above. After baking at 80°C under vacuum for 2 h, the nitrocellulose-bound samples were prehybridized in 5× Denhardt's (1× Denhardt's contains 0.02% BSA, 0.02% Ficoll, 0.02% polyvinylpyrrolidone), 5× SSC, 100 μg/ml tRNA at 37°C for 2 h, followed by hybridization with ^{32}P end-labeled oligo (dT) (Pharmacia Fine Chemicals, Piscataway, NJ) overnight at 37°C. Finally, the nitrocellulose was washed four times for 15 min each in 2× SSC at room temperature, prior to exposure to Kodak XAR-5 film at −70°C. Single dots (duplicates) were cut and counted using Cerenkov radiation to quantitate the bound radioactivity. The concentrations of total RNA from all of the tissues were adjusted, based on the results of the oligo(dT) hybridization assay, in order to utilize equal amounts of poly(A)+RNA for Northern blot analysis. The normalization of total RNA was verified by a second oligo(dT) hybridization.

IV. Northern Blot Analysis

Total RNA aliquots, normalized to equivalent amounts of poly(A)+RNA, were separated by electrophoresis on 1% agarose gels containing 0.60 M formaldehyde, and transferred to nylon membranes (Micron Separations, Inc., Westboro, MA) for hybridization with three different GJ cDNAs. (*a*) Human β_1-GJ cDNA: the human liver cDNA that codes for a 32 kD GJ protein (Kumar and Gilula, 1986). (*b*) Rat α_1-GJ cDNA: this is the cDNA clone isolated from a rat granulosa cell cDNA library, and it codes for a 43-kD GJ protein. (*c*) Mouse β_2-GJ cDNA: this cDNA clone was isolated from a mouse liver cDNA library (Nishi, M., N. M. Kumar, and N. B. Gilula, manuscript in preparation) and it codes for a 26-kD GJ protein. Hybridizations with the α_1- and β_2-cDNAs were performed in 50% formamide, 5× SSPE (1× SSPE contains 150 mM NaCl, 10 mM NaH_2PO_4, 1 mM EDTA-Na_2), 5× Denhardt's, 100 μg/ml tRNA, followed by washing in 0.1× SSC at 65°C. Hybridization conditions for the human β_1-GJ cDNA were similar, except that 40% formamide was used, followed by washing in 2× SSC at 55°C. Blots were processed by autoradiography at −70°C using Kodak XAR-5 film with an intensifying screen for 3 d. Signal intensities were quantified by densitometry using a LKB laser scanner (UltroScan IL; Bromma, Sweden). Multiple exposures were taken of the blot to allow for linearity in x-ray film response.

V. Screening of cDNA Libraries

A cDNA library constructed in lambda gt11 (Huynh et al., 1984) from rat granulosa cell mRNA was generously provided by Dr. Joanne Richards (Baylor College of Medicine, Houston, TX). Approximately 5 × 10^5 phages were screened at low stringency (20% formamide, 5× Denhardt's, 5× SSC, 100 μg/ml tRNA, 37°C; washing in 5× SSC at 45°C) using a synthetic oligonucleotide corresponding to the amino acid residues 201-215 of the endogenous α_1-GJ protein sequence (Beyer et al., 1987). Five hybridizing plaques were isolated, and then subcloned into the M13mp19 vector for DNA sequencing.

The cDNA clone coding for the mouse β_2-GJ protein was isolated from a mouse liver cDNA library (Nishi, M., N. M. Kumar, and N. B. Gilula, manuscript in preparation) using a synthetic oligonucleotide corresponding to amino acid residues 1-15 of the endogenous rat liver protein (Nicholson et al., 1987). The cDNA library was constructed from mouse liver mRNA according to the procedure of Gubler and Hoffman (1983). Sequence from a partial cDNA clone coding for a rat liver β_2-GJ has been reported (Nicholson and Zhang, 1988).

VI. DNA Sequence Analysis

α_1-GJ cDNA clones were excised from the bacteriophage vector and inserted into the Eco RI cloning site of M13mp19 for DNA sequencing by the modified chain termination method using the USB Sequenase kit (Tabor and Richardson, 1987). Internal sequence data were obtained by using synthetic oligonucleotides that were synthesized with a synthesizer (model 380A; Applied Biosystems, Inc., Foster City, CA). Sequence data were analyzed using PCGene software from IntelliGenetics (Palo Alto, CA).

VII. S1 Nuclease Protection Analysis

For detection of low abundance rat β_1-GJ transcripts, total RNA was hybridized in solution with a single-stranded 268-nt Kpn I fragment from a rat β_1-GJ cDNA (Kumar and Gilula, 1986). The probe was synthesized from a (+)-strand M13mp19 subclone using the large fragment of DNA polymerase I as described by Gimlich et al. (1988). The double-stranded extension product was digested with restriction endonuclease Kpn I (New England BioLabs, Beverly, MA) followed by electrophoretic purification of the antisense fragment on a 4% polyacrylamide gel (containing 7 M urea), and subsequently localized by autoradiography. After hybridization with total RNA (1 mg/ml) in 80% formamide, 0.4 M NaCl, 1 mM EDTA, 40 mM Pipes (pH 6.4), at 50°C, residual single-stranded probe was digested at 37°C with S1 nuclease (Bethesda Research Laboratories, Gaithersburg, MD) as described by Berk and Sharp (1977). DNA fragments protected by annealing with RNA were separated by electrophoresis in a 6% polyacrylamide gel containing 7 M urea. Bound radioactivity was detected by autoradiography at −70°C using Kodak XAR-5 film with an intensifying screen.

VIII. Thin-Section Electron Microscopy

Immediately after decapitation, the middle part of the d-2 and d0 uterine horns were initially fixed in situ by injection of 2.5% glutaraldehyde in 0.1 M cacodylate buffer (pH 7.4) into the muscle layer for 10 min. The tissue was then excised, cut into 1 × 2-mm pieces, and fixed in 2.5% glutaraldehyde in 0.1 M cacodylate for 60 min. at room temperature. After fixation, tissues were rinsed several times in 0.1 M cacodylate buffer, and then postfixed and embedded in epoxy resin as described previously (Gilula et al., 1978). Thin sections were cut with a diamond knife on a LKB Ultratome III, mounted on copper grids, post-stained with uranyl acetate and lead citrate, and examined with a Philips CM-12 electron microscope.

Results

Cloning a Rat Granulosa Cell α_1 GJ cDNA

A synthetic oligonucleotide probe corresponding to amino acid residues 210–215 of the rat α_1-GJ protein (Beyer et al., 1987) was used to screen and select an α_1-GJ cDNA from a rat granulosa cDNA library. The cDNA has been sequenced (Risek, B., N. M. Kumar, and N. B. Gilula, manuscript in preparation), and it is identical to the reported rat heart α_1-GJ cDNA (Beyer et al., 1987) in the 5′-untranslated and coding regions at the nucleotide level. However, the rat granulosa α_1-GJ cDNA differs in sequence from the rat heart α_1-GJ clone in the 3′ untranslated region. The rat granulosa cDNA codes for a protein with a predicted molecular mass of 43 kD that is identical to the size and amino acid sequence predicted from the heart cDNA (Beyer et al., 1987).

RNA Normalization and Peptide Antibody Specificities

For Northern blot analysis, the total RNA from each sample was "normalized" to a constant poly(A)+ RNA content using an oligo(dT) dot blot hybridization technique (see Materials and Methods and legend to Fig. 1 for details). An example of the RNA normalization for myometrial RNA samples is presented in Fig. 1.

The two peptide antibodies used for most experiments, termed β_1J and α_1J, were prepared against portions of the cytoplasmic loop of the β_1- and α_1-GJ proteins. The specificity of these antibodies was determined by immunoblot analysis (Fig. 2). Neither of the preimmune IgGs reacted with the native β_1- or α_1-GJ proteins. The β_1J antibody bound specifically to the 32-kD β_1-GJ protein that is present in rat liver, as well as to related multimers or large proteolytic fragments (>20 kD). The α_1J antibodies reacted specifically with the 43-kD GJ protein prepared from rat heart, and to its related multimers and proteolytic fragments. No cross-

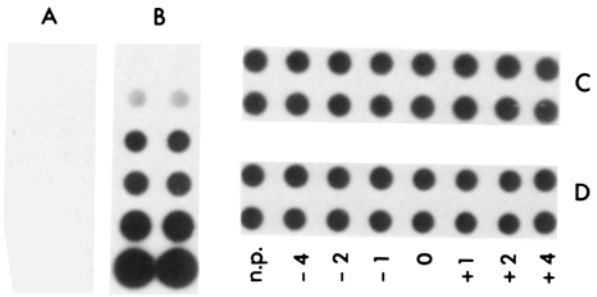

Figure 1. Normalization of total poly(A)+RNA by oligo(dT) dot blot hybridization. 1 μg of total RNA isolated from the myometrium at different stages of pregnancy was bound to a nitrocellulose membrane and hybridized with end-labeled oligo(dT)12–18. After autoradiography, the bound radioactivity was determined for individual samples (*dots*) by Cerenkov counting. (*A*) (from top to bottom) 0.3, 1, 3, 10, 30, and 100 μg yeast RNA. (*B*) (from top to bottom) 0.03, 0.1, 0.3, 1, 3, and 10 ng synthetic poly(A). (*C* and *D*) Total RNA was analyzed from the myometrium of nonpregnant (*n.p.*), d−4, d−2, d−1, d0, d+1, d+2, and d+4 pregnancy staged animals. In *C*, each sample represents 1 μg total RNA as determined by 260 nm absorbance, and the samples in *D* contain a normalized amount of total poly(A)+RNA.

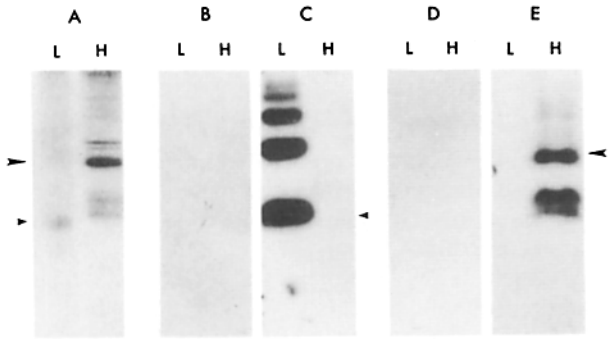

Figure 2. Immunoblot of isolated rat liver (β_1) and rat heart (α_1) gap junction proteins with β_1J and α_1J peptide antibodies. (*A*) Coomassie blue-stained SDS-PAGE of isolated GJ proteins from liver (*L*) and heart (*H*). (*B*) Immunoblot of a gel identical to that in *A*, incubated with affinity-purified preimmune IgG obtained from rabbit before immunization with β_1/KLH conjugate. (*c*) Identical immunoblot incubated with affinity-purified β_1J peptide antibodies. These antibodies strongly react with the 32-kD β_1 protein (*small arrowheads*) and its related multimers. There is no detectable cross-reaction with the α_1-GJ protein. (*D*) Immunoblot treated with affinity-purified IgG obtained from rabbit before immunization with α_1J/KLH conjugate. (*E*) Immunoblot incubated with affinity-purified α_1J antibodies. These antibodies react with the 43-kD α_1 protein (*large arrowheads*) as well as with the proteolytically related products of 34 and 32 kD. α_1J antibodies do not cross-react with the β_1-GJ protein.

reactivity was detected by immunoblotting with these two peptide antibodies and the α_1-, β_1-, and β_2-GJ proteins. In addition to immunoblot analysis, the antibody specificities were also confirmed by indirect immunofluorescence.

Gap Junction Expression in the Heart

A 3.6-kb transcript was detected in rat heart RNA by hybridization with the α_1-GJ cDNA probe (Fig. 3). The abundance of this transcript was not altered during different stages of pregnancy as determined by densitometric analysis. Also, no β_1 or β_2 transcripts were detected in the heart RNA samples after hybridization with the β_1- or β_2-GJ cDNAs (data not shown). These observations were confirmed by indirect immunofluorescence analysis using α_1J antibodies.

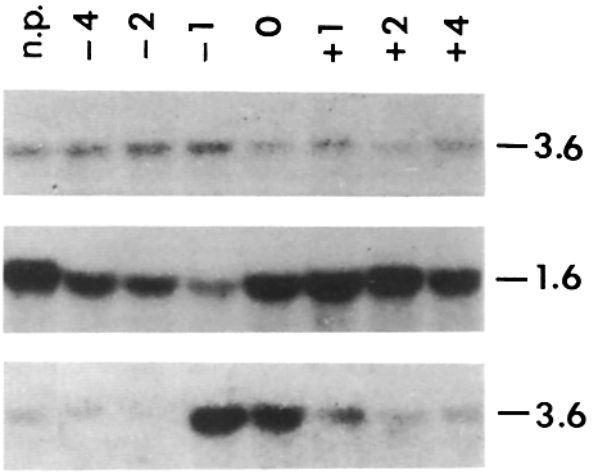

Figure 3. Northern blot analysis of β_1- and α_1-GJ transcripts in total RNA isolated from the rat heart, liver and ovary at different stages of pregnancy. Total RNA samples containing equal amounts of poly(A)+RNA were transferred to a nylon membrane and probed at high stringency (50% formamide, 37°C, washing in 0.1× SSC at 65°C) with the rat granulosa cell α_1-GJ cDNA (*top and bottom*), or the human liver β_1-GJ cDNA (*middle*). A transcript of 3.6 kb was detected in cardiac (*top*) and ovarian (*bottom*) samples with the α_1-GJ probe. In the liver (*middle*), a transcript of 1.6 kb was detected with the β_1-GJ probe. Signal intensities were analyzed by densitometry and are represented in Fig. 13.

In histological sections of unfixed heart tissue, the staining with α_1J antibodies was prominently localized to the intercalated discs, the cell surface specializations that contain GJs (Fig. 4, *left*). A typical punctate staining pattern was observed, which is consistent with the known discontinuous distribution of GJs within the myocardial intercalated discs. The density and intensity of the staining pattern in heart samples taken from nonpregnant animals were quite similar to that observed in tissues from pregnant animals. Fig. 4 contains sections from non-pregnant, d-2, d0, and d+2 animals. No differences were detected in the staining pattern at various stages of pregnancy. Thus, both α_1-GJ transcripts and the corresponding protein were not altered during pregnancy.

Gap Junction Expression in the Liver

An analysis of β_1-GJ transcripts in liver during different stages of pregnancy using the human liver β_1-GJ cDNA probe is shown in Fig. 3. The size of the detected transcript was 1.6 kb. Relative to the transcript level in nonpregnant animals, which was defined as "1," the transcript abundance was significantly reduced in pregnant animals during the prepartum period (-4, -2, and -1 d before delivery), reaching the lowest value of 0.42 at d-1. On the day of parturition (d0), 3–6 h after delivery, the abundance was decreased to 0.8 of the nonpregnant level. In postpartum animals at d+1, the β_1-GJ transcript abundance reached the nonpregnant sam-

ple level. A slight decrease was consistently observed at d+4. With the same hybridization conditions, no α_1 or β_2 transcripts were detected in the liver RNA after treatment with the α_1 or β_2-GJ cDNAs (data not shown).

The observed pre- and postpartum changes in liver β_1-GJ transcripts were supported by indirect immunofluorescence using the β_1J peptide antibodies. Fig. 4 (*right*) contains sections of liver from nonpregnant, d-2, d0, and d+2 animals treated with the β_1J antibodies. There was prominent punctate staining at the cell borders with comparable intensity and distribution in the nonpregnant, d0 and d+2 specimens. In contrast to nonpregnant and postpartum liver, in d-2 samples the staining was patchy, with only a few regions showing intense pericellular fluorescence (Fig. 4 *h*). In other regions, the amount of staining was much lower; the immunofluorescence was detectable as small faint spots. Similar results were obtained in samples from d-4 and d-1, in agreement with the decrease in junctional transcript levels observed at these stages using Northern blot analysis. Thus, both the β_1-GJ transcripts and the corresponding protein appeared to be downregulated in the liver of prepartum rats, relative to nonpregnant and postpartum animals.

Gap Junction Expression in the Ovary

Hybridization of total RNA from ovaries using the α_1-GJ cDNA resulted in detection of a 3.6 kb transcript (Fig. 3). Using the same stringency conditions, hybridization with the β_1-GJ and β_2-GJ cDNAs failed to detect any transcripts. The abundance of the 3.6-kb transcript was significantly altered during pregnancy, increasing from essentially nonpregnant levels at d-4 and d-2 to peak at d-1 (6.7-fold over the nonpregnant level). The level declined rapidly at d0 (2.5 times), reached the non-pregnant level again at d+2, and remained constant at d+4.

These observations were correlated with changes in the immunostaining of GJ protein in the ovaries. Immunofluorescence analysis on the nonpregnant ovary using the α_1J antibodies indicated extensive staining between granulosa cells of the preovulatory ovarian follicles (Fig. 5 *a*). In some regions this staining was punctate, and in other areas it formed a continuous cell surface rim, consistent with very high levels of GJ protein. In addition, the theca externa surrounding the follicles contained some punctate staining, as well as the stromal cells of the postovulatory corpora lutea (Fig. 5 *b*). In ovaries from animals at different stages of pregnancy, there was no detectable alteration in the intensity or density of GJ staining in the theca externa or in the preovulatory follicles. In contrast, there were considerable changes in the staining of the stromal regions. In the nonpregnant specimen (Fig. 5 *c*), there was a low level of immunolabeling. At stages d-4 and d-2, the staining pattern was more prominent (Fig. 5 *d*), and by d0 many of the stromal cells contained intense fluorescent spots (Fig. 5 *e*). The staining density decreased subsequently to reach almost the nonpregnant level at d+2 (Fig. 5 *f*). Thus, the temporal modulation of ovarian stroma α_1-GJ protein is consistent with the results obtained by Northern blot analysis.

Gap Junction Expression in the Uterus

The Myometrium. Hybridization of myometrial RNA with the α_1-GJ cDNA identified a single 3.6-kb band (Fig. 6), identical to that found in the heart and ovary RNA. The abundance of this transcript varied markedly during pregnancy. In addition, the temporal pattern of expression was strikingly similar to that previously observed in the ovary. At 4 d before birth (d-4), the transcript level was comparable to that in nonpregnant animals. By d-2, the level had increased 2.3 times over the nonpregnant level, reaching a maximal value at d-1 where transcripts were 5.5 times that found in nonpregnant animals. At d0, the transcript abundance rapidly declined (3.6-fold over nonpregnant level), and, at d+1, was 2-fold greater than the nonpregnant sample. The level increased slightly at d+2 relative to d+1 (data from three independent experiments) and declined at d+4 to the nonpregnant state. No β_1-GJ transcripts were detected in the myometrial RNA samples by Northern blot analysis.

The sizable enhancement of α_1-GJ transcripts in the myometrium at d-1 was paralleled by immunofluorescence observations on α_1-GJ protein in uterine sections. With the α_1J antibodies, the nonpregnant myometrium contained occasional small fluorescent spots between the smooth muscle cells (Fig. 7 *b*). This staining pattern was similar in the d-1 and d+1 samples, and there was fluorescence between connective tissue cells and around the periphery of blood vessels, which are located between the circular and longitudinal muscle layers. However, a dramatic change was observed in tissue sections taken from animals 3 h after parturition (d0) (Fig. 7, *c* and *f*). Myometrial cells contained large numbers of brightly fluorescent spots along their borders, easily visible even at low magnification. This staining was distributed between the cells in the inner circular muscle layer, the outer longitudinal muscle layer, and in the decidual cells of the endometrium. (After implantation, stromal cells are transformed to decidual cells.) In the d0 specimen the fluorescent spots were frequently aligned in rows along the long axis of muscle fibers in the circular muscle layer (Fig. 7 *f*). Some fluorescence was also detected at the serosal surface. However, the staining was, by far, most prominent in the circular muscle layer. These findings suggested that an increase in the α_1-GJ transcript level on d-1 was followed by a rapid increase in the α_1-GJ protein on the day of parturition. No staining was observed in the endometrial epithelium using the α_1J antibodies.

The presence of myometrial GJs at d0 localized in the inner circular smooth muscle layer by indirect immunofluorescence was confirmed by thin-section EM. Myometrial GJs, with a typical septilaminar structure, were found predominantly between cells in the circular smooth muscle layer (Fig. 7 *g*). Immediately after delivery, GJs were increased in number and in size, compared with nonpregnant uterus (data not shown).

The Endometrium. Total RNA was isolated from the endometrium at four different stages of gestation. The endometrial samples also varied in total RNA content but were normalized to contain the same amount of poly(A)+RNA. Although there were no detectable signals for β_1-GJ transcripts on Northern blots of endometrial RNA, β_1-transcripts were detected by S1 nuclease protection (Fig. 8, lane *4*). Hybridization with the α_1-GJ probe resulted in the detection of a 3.6-kb transcript (data not shown). Because the temporal distribution was comparable to that found in the myometrium at the same stages of pregnancy, the α_1-GJ transcripts that were detected in the endometrium may repre-

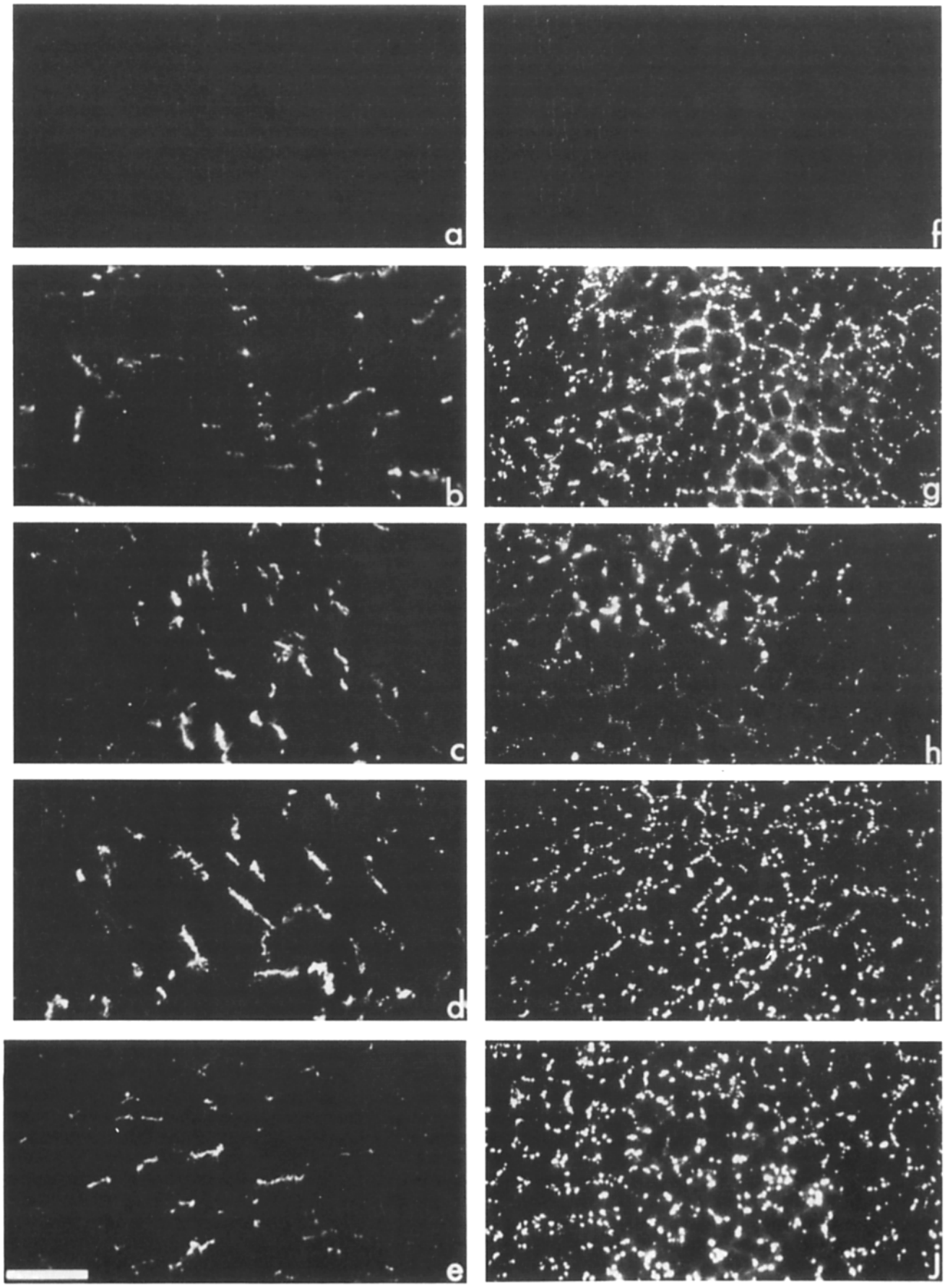
a
f
b
g
c
h
d
i
e
j

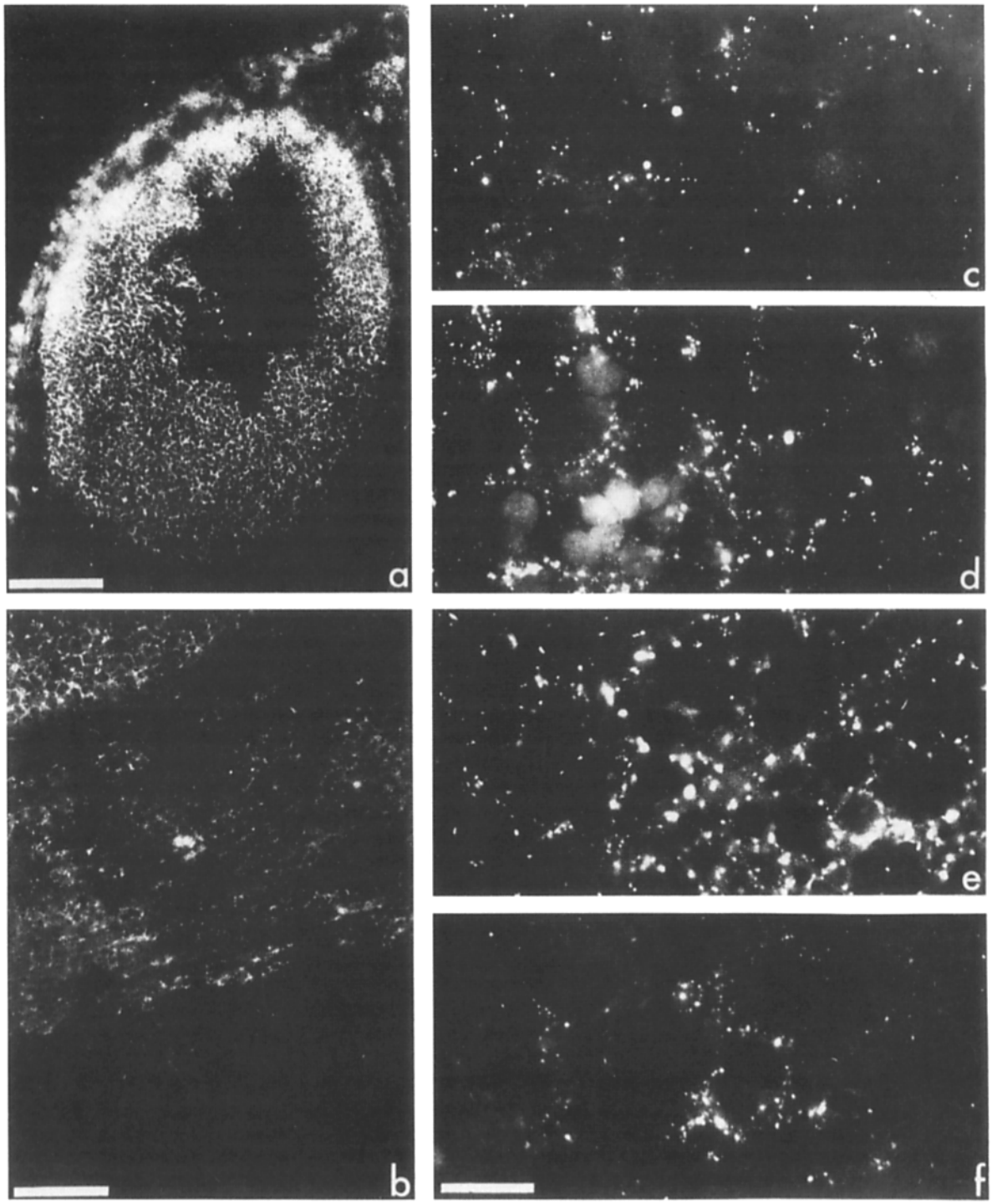

Figure 5. Immunohistochemical localization of α_1 antigen in frozen sections of ovary with α_1J antibodies. Bound antibody was detected with FITC-goat anti-rabbit IgG. (*a*) Preovulatory ovarian follicle from nonpregnant animal with extensive cell surface fluorescence outlining the follicular granulosa cells. Bar, 100 μm. (*b*) Three regions of nonpregnant ovarian tissue, follicle cells (*top left corner*), theca externa (below follicle), and stroma of postovulatory corpus luteum (*bottom right*). At this magnification, α_1 antigen is detectable in the follicle and theca externa, but not in the stromal region. Bar, 50 μm. (*c–f*) Stromal regions of postovulatory corpora lutea in ovaries from animals at different stages of pregnancy (*c*, nonpregnant, *d*, d−2; *e*, d0; *f*, d+2). Bar in *f*, for *c–f*, 20 μm.

Figure 4. Immunohistochemical localization of α_1 and β_1 antigens in frozen sections of heart and liver with α_1J and β_1J antibodies during pregnancy. Heart and liver sections were treated with α_1J (heart), β_1J (liver), or corresponding preimmune antibodies. Antibody binding to gap junction antigens was detected with FITC-goat anti-rabbit IgG. Bar, 50 μm. (*a–e*) Heart sections treated with preimmune (*a*) and with α_1J antibodies at different stages of pregnancy (*b*, nonpregnant; *c*, d−2; *d*, d0; *e*, d+2). (*f–j*) Liver sections treated with preimmune (*f*) and with β_1J antibodies at different stages of pregnancy (*g*, nonpregnant; *h*, d−2; *i*, d0; *j*, d+2).

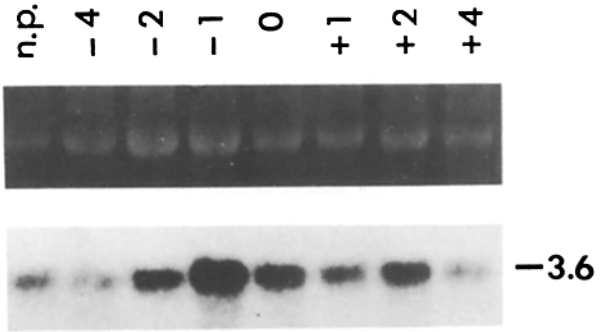

Figure 6. Northern blot analysis of α_1-GJ transcripts in total RNA isolated from the myometrium at different stages of pregnancy. Samples of total RNA containing equal amounts of poly(A)+RNA were hybridized at high stringency (50% formamide, 37°C, washing in 0.1× SSC at 65°C) using the rat granulosa α_1-GJ cDNA probe, and visualized by autoradiography. Ethidium bromide staining of myometrial total RNA (18S rRNA) (*top*). Varying levels of a 3.6-kb transcript were detected in the myometrial samples (*bottom*). Signal intensities were quantified by densitometry and are presented in Fig. 13.

sent cross-contamination with myometrium and the endometrial decidua (transformed stromal cells of the endometrium), where the α_1-GJ antigen was detected by immunofluorescence.

Hybridization of endometrial total RNA with the β_2-GJ probe under high stringency conditions resulted in detection of a 2.8-kb transcript (Fig. 9). The transcript abundance varied with the stage of pregnancy, but was not detectable in nonpregnant samples. For this reason we defined the signal intensity at d0 as "1" to compare relative prepartum changes. At d-4, the transcript abundance was 2.0 times the value at d0, reaching maximal level of 2.4 times at d-2 with a subsequent decrease (0.5 times the value at d0) at d-1. Postpartum analysis of the endometrial β_2-GJ transcript could not be carried out due to an enormous decrease in the endometrial mass after delivery. A similar profile of endometrial β_2-GJ transcripts was observed when analyzed in whole uterus without the implantation sites (data not shown).

Variable amounts of GJ antigen were detected in the endometrial epithelium by immunohistochemical treatment of uterine sections with β_1J antibodies. In nonpregnant samples, a low level of antigen was localized in small discrete spots along the lateral borders of the cells, and in the regions adjacent to the endometrial stroma (Fig. 10 *a*). However, a pronounced staining within the epithelium was observed on d-2 (Fig 10 *b*), declining to very low levels at d0 and d+1 (Fig. 10, *c* and *d*). At d-2, the stained regions were elongated, compatible with an increase in the size of individual GJ plaques. These findings were confirmed by EM on uterine thin sections. At d-2, the endometrial GJ plaques were much larger in size (Fig. 10 *e*), as compared with nonpregnant tissue where only small GJs were found (data not shown). Thus, the observations made by immunofluorescence are consistent with the results obtained by EM.

Because β_2-GJ transcripts were more abundant than β_1-GJ transcripts in the endometrium, the results obtained by immunofluorescence suggested that the β_1J antibodies, raised against an epitope on the rat liver β_1-GJ protein, cross-reacted primarily with β_2-GJ protein in the endometrial epithelium. To explore this possibility, material from the liver and uterus was treated with two additional antibodies. One of these, β_1S was prepared to a synthetic peptide sequence in the carboxy-terminal region of the β_1 protein (Milks et al., 1988). Because the β_2-GJ protein (26 kD) has a much shorter carboxy terminus than the β_1-protein (32 kD), it does not include a region homologous to the S region, and consequently should not bind the β_1S antibodies. The second one, β_2J, is an antibody prepared against a synthetic peptide to the cytoplasmic loop region of the β_2-GJ protein. Although there is some potential antigenic homology between the β_1J and β_2J sequences, the two antibodies clearly discriminated between the β_1 and β_2 gene products by immunoblotting of SDS-denatured proteins (Fig. 11). Under these conditions, the β_1 protein was detectable in nonpregnant liver, but not in the d-2 endometrial epithelium (Fig. 11 *B*). However, the β_2 protein was detected in both liver (low levels) and endometrial epithelium samples (Fig. 11 *C*). Based on the densitometric analysis of bands shown in Fig. 11 *C* (lanes *L* and E_1), β_2 protein in the d-2 endometrium was 3.5-fold greater than in liver. Because the amount of liver material applied was eight times the amount of d-2 endometrial sample (50 vs. 6.25 μg), the relative abundance of endometrial β_2 protein can be estimated to be 28-fold greater than that present in nonpregnant liver.

When d-2 frozen sections of uterus were treated with the β_1S antibodies, the level of staining was significantly reduced (Fig. 12 *d*), compared with the β_1J antibodies (Fig. 12 *b*). There was also a slight decrease in labeling density in rat liver frozen sections with the β_1S antibodies, compared with the β_1J antibodies (Fig. 12, *a* and *c*). This may indicate that the β_1J antibodies were interacting with two types of liver GJ protein (β_1 and β_2), whereas the β_1S antibodies reacted only with the β_1-GJ protein. Analysis by immunofluorescence of liver sections from animals at different stages of pregnancy showed similar changes using both the β_1J and the β_1S antibodies, except that the degree of labeling with the β_1S antibodies was consistently lower (data not shown). Finally, efforts to discriminate between the β_1 and β_2 proteins by immunofluorescence using the β_1J and β_2J antibodies have been ambiguous. For example, both β_1J and β_2J antibodies detected high levels of antigen in both liver and endometrial epithelium sections (Fig. 12, *a*, *b*, *e*, and *f*). However, all of the data combined (mRNA, protein, and immunofluorescence) indicated that most of the antigen detected by the β_1J antibody in the endometrium was, in fact, the β_2 protein, and that this was the most abundant GJ protein in the endometrial epithelium.

Gap Junction Transcript Abundance Relative to Poly(A)+ RNA Levels during Pregnancy

To determine if the alterations in GJ mRNA levels during pregnancy were unique for the junction mRNAs or were related to a general fluctuation of poly (A)+ RNA, the two values were determined in different organs during pregnancy and compared directly (Fig. 13).

Although the level of cardiac α_1-GJ mRNA was not altered during pregnancy (the observed changes were within experimental error), there was a slight increase in the steady-state level of total poly(A)+ RNA at d-1 and d0, reaching a

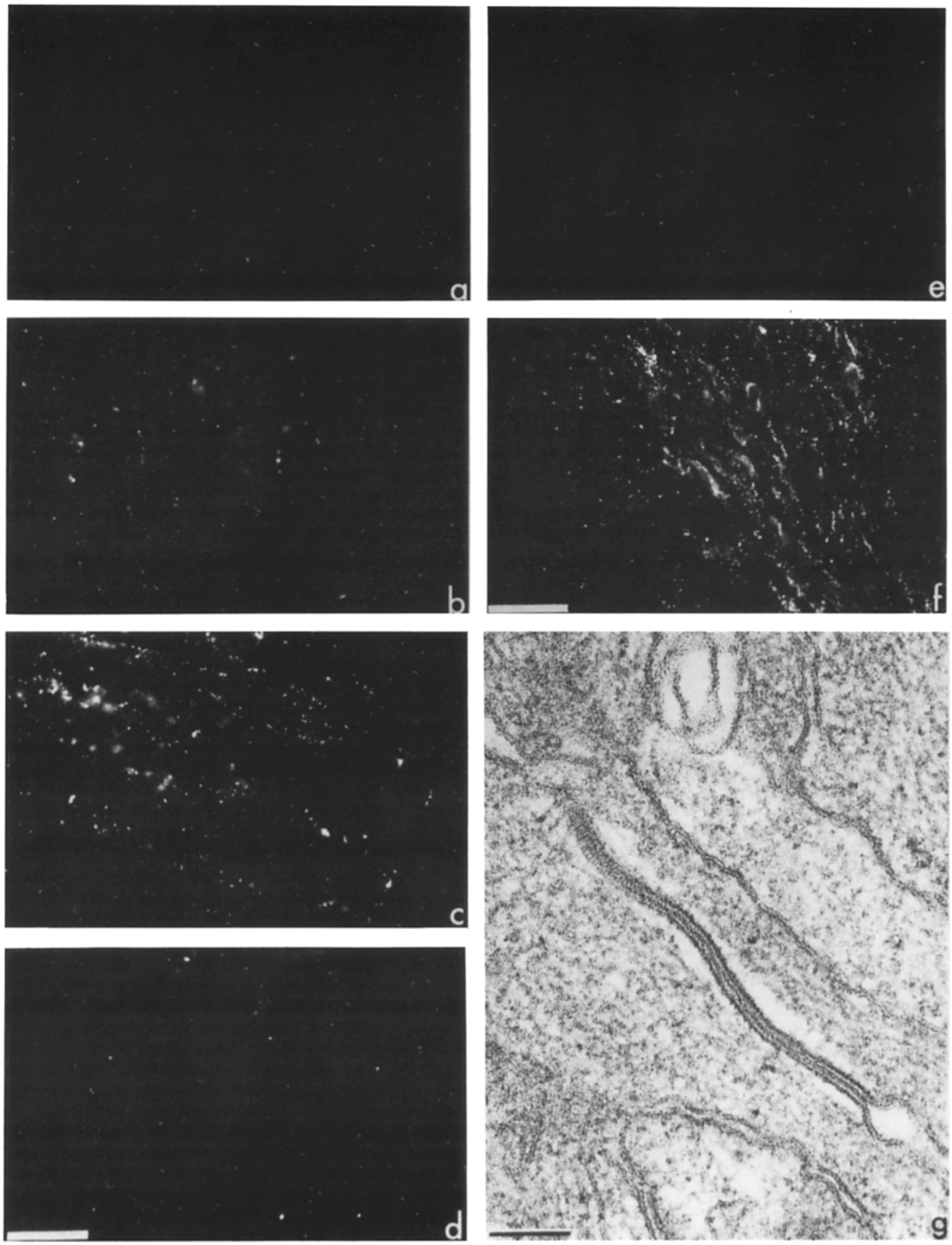

Figure 7. Immunohistochemical localization of α_1-GJ antigen in frozen sections and thin-section EM of uterine myometrium. (*a–d*) Histological sections through the circular muscle layer of the uterine myometrium at different stages of pregnancy treated with α_1 antibodies. Bound antibodies were detected with FITC goat anti-rabbit IgG. (*a*), nonpregnant; *b*, d−1; *c*, d0 (3 h after birth); *d*, d+1). Bar, 20 μm. (*e*) Section through the circular muscle layer of the myometrium and stromal layer of the endometrium in a nonpregnant uterus. (*f*) Section through the circular muscle layer of the myometrium, decidua and epithelium of the endometrium on d0. Note staining with the α_1J antibodies in smooth muscle and endometrial decidua region, but not in the endometrial epithelium (*bottom left*). Bar for *e* and *f*, 50 μm. (*g*) Thin-section electron micrograph of a gap junction between two smooth muscle cells in the circular muscle layer on d0 (3 h after birth). Bar, 0.1 μm.

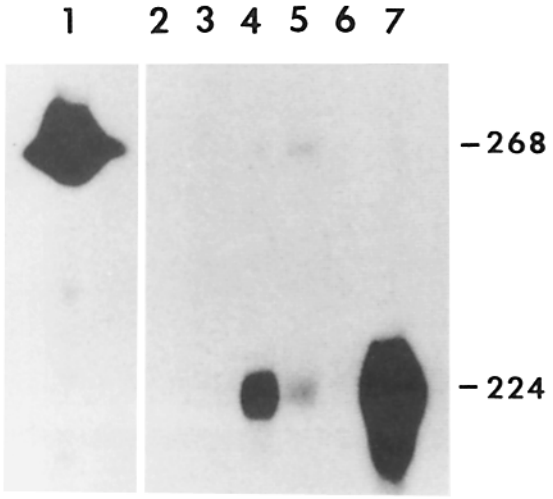

Figure 8. Detection of β_1-GJ transcripts in total RNA isolated from different tissues by S1 nuclease protection assay. A 268-base single-stranded rat liver β_1-GJ cDNA fragment was annealed to completion with 30 μg total RNA. After S1 nuclease digestion, a protected fragment of 224 nucleotides was detected in RNA from the endometrium (lane *4*), myometrium (lane *5*) and liver (lane *7*), but not in the heart (lane *3*) and ovarian (lane *6*) samples. Lane *1* contains the probe; lane *2*, 30 μg of tRNA.

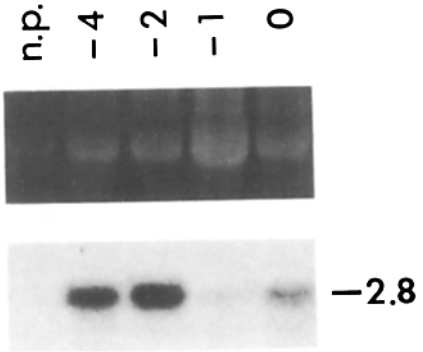

Figure 9. Northern blot analysis of the β_2-GJ transcript in total RNA isolated from the endometrium at different stages of pregnancy. Samples of total RNA containing equal amounts of poly(A)+RNA were hybridized at high stringency (50% formamide, 37°C, washing in 0.1× SSC, 65°C) using the liver β_2-GJ cDNA and visualized by autoradiography. Ethidium bromide staining of total RNA (18S rRNA) (top). Varying amounts of a 2.8 kb β_2-transcript were detected in the RNA samples with the β_2-GJ cDNA probe (bottom). Signal intensities of 2.8-kb transcript were analyzed by densitometry and are presented in Fig. 13.

maximum at d+1 (1.45-fold increase over nonpregnant sample level). At d+2, the RNA returned to the nonpregnant level, and remained constant at d+4. Thus, the α_1-GJ mRNA level was not detectably influenced by changes in the poly (A)+RNA abundance in the heart during pregnancy. In liver, the profile of total poly(A)+ RNA was essentially the same as observed for β_1-GJ mRNA (Fig. 13). Therefore, the change in liver β_1-GJ transcripts was most likely due to a general alteration of poly(A)+ RNA levels in the liver during pregnancy.

In contrast to liver, the observed modulation of ovarian α_1-GJ mRNA was probably not due to changes in poly(A)+ RNA content. The steady-state level of ovarian poly(A)+ RNA gradually increased from d-4, reaching a high value of 1.7 at d+4, whereas the α_1 mRNA level reached a maximum at d-1 (Fig. 13). Thus, this significant difference in temporal profiles between α_1-GJ mRNA and total poly(A)+ RNA indicates that there was a specific modulation of ovarian α_1-GJ transcripts during different stages of pregnancy.

The temporal expression of myometrial α_1-GJ transcripts also appeared to be modulated in a specific manner, as the profile differed markedly from that obtained with total poly(A)+ RNA (Fig. 13). During all three prepartum stages examined, the concentration of total poly(A)+ RNA was ~50% less than the pregnant level. After parturition, the abundance increased gradually, reaching the nonpregnant level at d+4. Conversely, the poly(A)+ RNA concentration in the endometrium decreased during the prepartum period to a minimum of 0.4 times at d-1; a decrease at d-1 was also observed for the β_2-GJ mRNA. However, comparison of the β_2-GJ mRNA profile with that for endometrial total poly(A)+RNA indicated that there was a specific modulation of the β_2-GJ transcript. Whereas the relative concentration of β_2-GJ mRNA increased about twice over the value at d0, the abundance of poly(A)+RNA was 0.7 times at the same time.

Discussion

In this study, the expression and distribution of three different GJ gene products has been examined in various tissues using specific cDNA probes and peptide antibodies during different stages of pregnancy. Several relevant observations have resulted from this analysis. First, a cell-specific modulation of the α_1-GJ transcripts has been observed in the myometrium and ovary during pregnancy. Whereas the expression of α_1-GJs in the myometrium and ovary was regulated in a similar manner, the heart α_1-GJs were expressed constitutively. Second, the α_1-GJ antigen was localized in the circular and longitudinal smooth muscle layer of the myometrium, in the endometrial decidua, in the ovarian stroma, and in the heart. Third, identification, transcript modulation, and cellular localization of the β_2-GJs were described in the endometrial epithelium. Fourth, a modulation of β_1-GJ transcripts and protein was observed in the liver during the pre- and postpartum period of pregnancy. Finally, it was possible to determine temporal differences for maximal myometrial α_1- and endometrial β_2-GJ expression during pregnancy.

In pregnant animals, the highest concentration of α_1-GJ mRNA was found in the myometrium and ovaries 1 d before delivery (d-1), resulting in a maximal increase of α_1-GJ structures at d0 as determined by immunofluorescence. Because there was no detectable alteration of α_1-GJ expression in the heart, these findings indicate that there was a tissue-specific modulation of the α_1-GJ transcript in the myometrium and ovary. In the myometrium, both the outer longitudinal and inner circular smooth muscle layers contained α_1-GJ protein, with a more prominent immunostaining in the circular muscle layer. No β_1-GJ transcripts were detected in endometrial RNA by Northern blot analysis, but

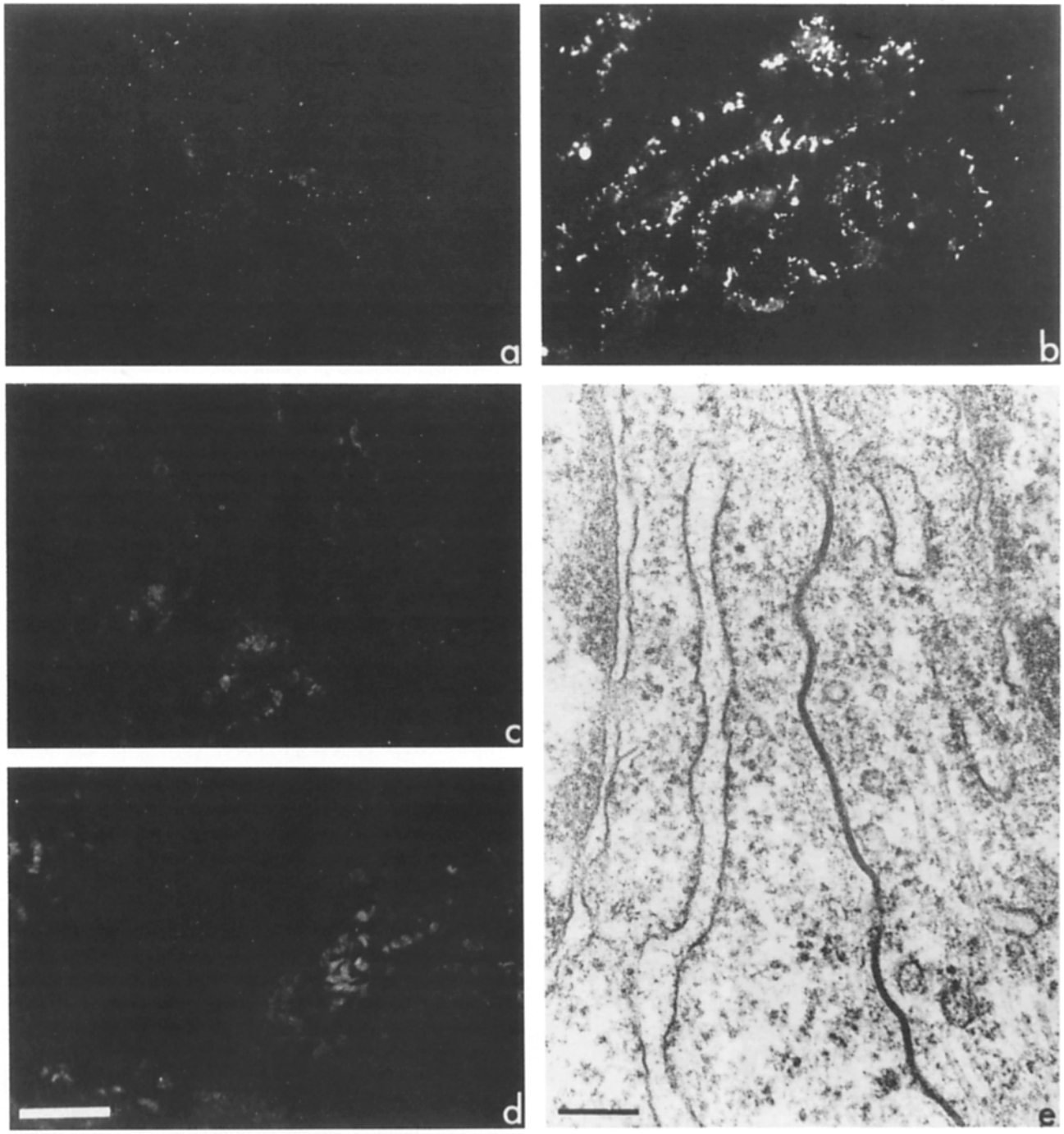

Figure 10. Immunohistochemical localization of β_1-related antigen in frozen sections and thin-section EM of uterine endometrium. (*a–d*) Histological sections through the epithelium and stroma (decidua) of the uterine endometrium at different stages of pregnancy, treated with the β_1J antibodies. The endometrial epithelial cells contain detectable gap junction antigen in nonpregnant (*a*) and prepartum (*b*) samples. Bound antibodies were detected with FITC-goat anti-rabbit IgG. (*a*, nonpregnant; *b*, d−2; *c*, d0; *d*, d+1). Bar, 50 μm. (*e*) Thin-section electron micrograph of an extensive gap junction between two endometrial epithelial cells on d−2. Bar, 0.2 μm.

they were detectable using the more sensitive S1 nuclease protection assay. Clearly, the most abundant transcript in the endometrium was 2.8 kb, and it was detected using the β_2-GJ cDNA probe.

The immunofluorescence observations with β_1J and β_2J antibodies indicated that both β_1- and β_2-GJ proteins were exclusively localized in the endometrial epithelium. This observation was supported by both the Northern blot analysis and the S1 nuclease protection assay. However, application of β_1J, β_1S, and β_2J antibodies provided a unique discrimination between the β-related antigens in the endometrium. These observations suggested that the β_1J antibodies also interacted with the cytoplasmic J loop of the β_2-GJ protein, where 5 of 15 amino acids are identical in the two proteins.

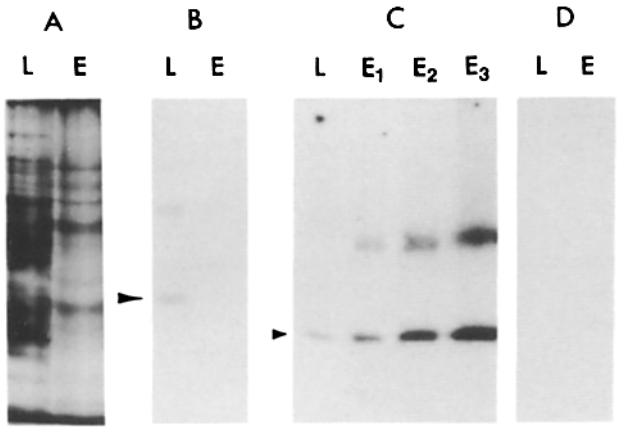

Figure 11. Immunoblot of NaOH-insoluble rat liver and rat endometrium homogenates with β_1J and β_2J peptide antibodies. (*a*) Coomassie blue-stained SDS-PAGE of nonpregnant liver (*L*, 50 μg) and d−2 endometrium samples (*E*, 25 μg). (*b*) Immunoblot of a gel identical to that in A, incubated with affinity-purified β_1J peptide antibodies. A polypeptide of 32 kD (*large arrowhead*), as well as the 46-kD dimeric form, was detected in rat liver, but not in the endometrial sample. (*c*) Immunoblot of a gel identical to that in *A*, with different amounts of endometrial material (E_1, 6.2 μg; E_2, 12.5 μg; E_3, 25 μg), treated with affinity-purified β_2J peptide antibodies. These antibodies bound to a polypeptide of 26 kD (*small arrowhead*) present in rat liver (*L*) and d-2 endometrium (*E*). In addition, an aggregated or dimeric form of the protein was detected in liver (43 kD) and endometrium (38 kD) (*d*) Immunoblot treated with affinity-purified IgG obtained from rabbit before immunization.

The apparent cross-reactivity was most likely due to the presence of a conformationally similar epitope in these two proteins in frozen sections, because the β_2-GJ protein was not detected on immunoblots of d-2 endometrial samples using β_1J antibodies. Thus, even though peptide antibodies may provide exquisite sequence specificity on SDS-denatured antigens (by immunoblotting), the same antibodies may be capable of binding to conformationally related epitopes in other proteins under immunohistochemical conditions where the antigens are not SDS denatured. Consequently, stringent criteria and appropriate controls must be applied when determining the specificity of "sequence-specific" peptide antibodies under the conditions applied for immunohistochemistry. This potential cross-reactivity is important to consider in the context of two recent studies that have reported the immunofluorescence localization of β_1-GJ protein in the endometrial epithelium of the rabbit (Winterhager et al., 1988) and the rat (Beyer et al., 1989).

In contrast to the elevation of α_1-GJ transcripts in the myometrium, the increase in endometrial β_2-GJ transcripts occurred one day earlier, reaching a maximal concentration at d-2. The maximal immunostaining of myometrial α_1-GJ protein was obtained immediately after delivery at d0, whereas the peak of β_2-GJ structures in the endometrium was observed 2 d before birth. At birth, the β_2-GJ antigen was barely detectable in the endometrium by immunofluorescence using β_1J antibodies. These results not only document that two different GJ proteins are abundant in the pregnant uterus, but they also demonstrate that they are regulated differently.

The differential modulation of the α_1 and β_2 gene products that has been reported here is interesting to consider in the context of circulating ovarian steroid hormone concentrations in the pregnant rat. At the onset of pregnancy, the progesterone concentration is high and begins to fall progressively between day 15 of gestation and term (Puri and Garfield, 1982; Saito et al., 1985). During this period, β_2-GJ antigen is expressed in the endometrial epithelium with an absence of α_1-GJ antigen in the smooth muscle layer of the myometrium. At the same time, the estrogen level is low

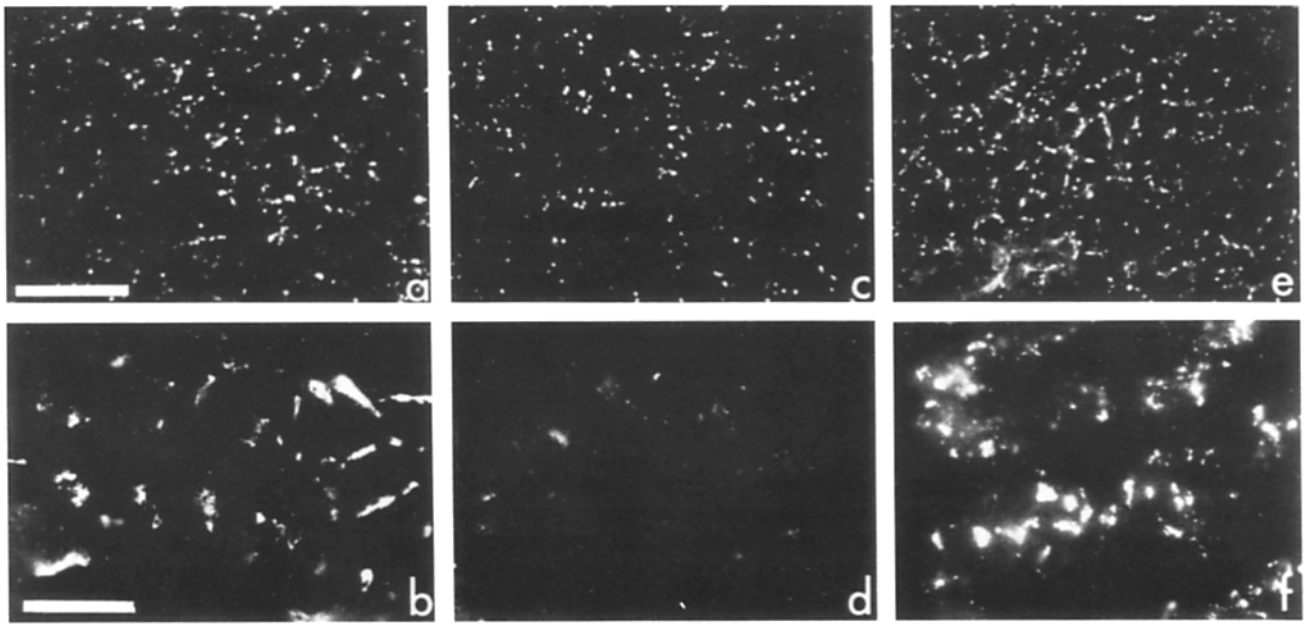

Figure 12. Immunohistochemical localization of β_1 and β_2 gap junction and antigens in frozen sections of non-pregnant liver and d-2 uterine endometrial epithelium. Bound antibodies were detected with FITC-goat anti-rabbit IgG. Sections of non-pregnant liver (*top*) and d-2 endometrial epithelium (*bottom*) were treated with β_1J (*a* and *b*), β_1S (*c* and *d*) and β_2J (*e* and *f*) peptide antibodies. Bar in *top*, 50 μm; in *bottom*, 20 μm.

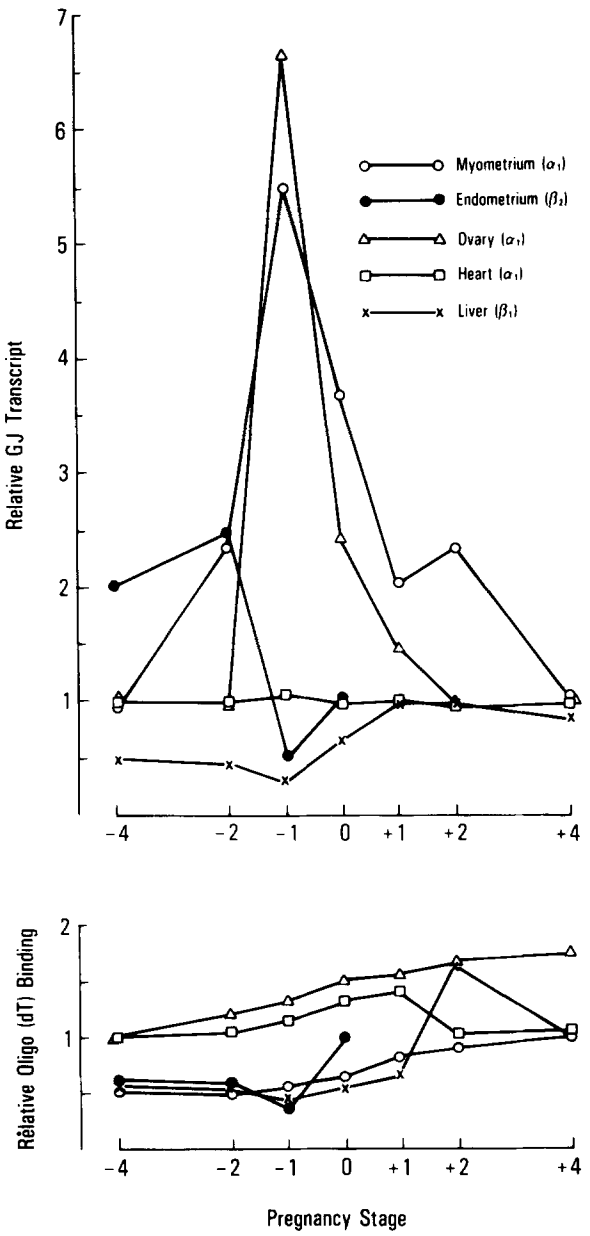

Figure 13. Relative GJ transcript abundance and total poly(A)+ RNA during different stages of pregnancy. (*Top*) β_1-, α_1- and β_2-GJ transcripts detected by Northern blot analysis using corresponding cDNA probes were quantified by laser scan densitometry. The peak area corresponding to the transcriptional signal intensity was integrated and normalized to the level of the non-pregnant sample; that level was defined as "1." Because the β_2-GJ transcript was not detectable in the non-pregnant uterus, the value for that transcript at d0 was defined as "1." The diagram represents changes in transcript abundance relative to the non-pregnant state for heart, liver, ovary, and myometrium, and to d0 for the endometrium. (*Bottom*) This diagram contains profiles of the abundance of poly A(+) RNA during the different stages of pregnancy in the organs that were analyzed. Poly A(+) RNA was determined by oligo (dT) binding to total RNA samples.

in maternal tissues. Approaching delivery, progesterone declines to an undetectable level resulting in an increase in the estrogen/progesterone ratio, and one observes during this period the formation of α_1-GJs in the myometrium and ovaries with concomitant regression of β_2-GJs in the endometrial epithelium. Thus, it appears that the synthesis of endometrial β_2-GJs may be at least partly under the control of ovarian progesterone (progesterone from fetal origin may be additionally involved), whereas the formation of myometrial and ovarian α_1-GJs appears to be an estrogen-dependent process. Although the physiological significance of the ovarian α_1-GJ changes observed in corpora lutea is not known, it may be related to the process of luteolysis, i.e., regression of the corpus luteum after pregnancy. In contrast to the ovary, much more is known about the primary target organ, the myometrium, where formation of α_1-GJs appears to be a necessary prerequisite for synchronized muscle contraction during delivery (Garfield et al., 1977). Conversely, the preceding loss of endometrial β_2-GJs on d-1 may be, in part, involved in the process of uncoupling the fetal-maternal communication to facilitate birth at the same time that the myometrial α_1-GJs reach a maximum to permit a synchronized contraction of the uterine wall.

Although a specific modulation of GJ transcripts in steroid hormone responsive tissues has been shown in this study, the mechanisms whereby these effects are exerted in a temporal and cell-specific manner are not known. Because transcript analysis and cell-specific localization of assembled GJ proteins are restricted to steady-state analysis of corresponding mRNA concentrations, the sites of action of these regulatory controls remain to be determined. A priori, the observed transcript modulation may be a consequence of an altered rate of gene transcription, altered stability of the primary transcript or processing intermediates, or differential mRNA turnover (Darnell, 1982). However, based on current concepts of steroid hormone action (for reviews, see Yamamoto, 1985; Evans, 1988), it is likely that an increase in GJ transcripts results, in part, from a hormonally induced increase in the rate of transcription of the specific gene(s). Therefore, to understand the potential hormonal regulation of the GJ genes, it will clearly be important to identify the potential hormone-responsive elements in these genes.

This study of the pregnant animal model has provided evidence for the differential modulation of three members of the GJ gene family. Consequently, this biological model offers a unique opportunity to study processes underlying hormonal, developmental, and cell-specific gene expression of a group of important membrane proteins.

The authors are grateful for the outstanding technical assistance of Jessica Van Leeuwen, Matt Haynes, Venetia Collier, and Dan Jones, the excellent secretarial support from Cheryl Negus, and the constructive suggestions and criticisms from Dr. Bill Beers during the course of this study. We are grateful to Dr. Joanne Richards for providing the rat granulosa library. We also appreciate the opportunity to utilize peptide antibodies from Dr. Linda Milks, the β_2 cDNA clone from Dr. Miyuki Nishi, and heart gap junction protein from Dr. Mark Yeager.

This work was supported by National Institutes of Health grants GM-37904 (to N. B. Gilula), EY-06884 (to N. M. Kumar), and GM-37907 (to N. B. Gilula and N. M. Kumar).

Received for publication 12 July 1989 and in revised form 17 October 1989.

References

Berk, A. J., and P. A. Sharp. 1977. Sizing and mapping of early adenovirus mRNAs by gel electrophoresis of S1 endonuclease digested hybrids. *Cell.* 12:721–732.

Beyer, E. C., L. Paul, and D. A. Goodenough. 1987. Molecular cloning of

cDNA for connexin 43, a gap junction protein from rat heart. *J. Cell Biol.* 105:2621–2629.

Beyer, E. C., J. Kistler, D. L. Paul, and D. A. Goodenough. 1989. Antisera directed against connexin 43 peptides react with a 43-kD protein localized to gap junctions in myocardium and other tissues. *J. Cell Biol.* 108:595–605.

Burghardt, R. C., R. L. Matheson, and D. Gaddy. 1984. Gap junction modulation in rat uterus: I. Effects of estrogens on myometrial and serosal cells. *Biol. Reprod.* 30:239–248.

Chirgwin, J. M., A. E. Przybyla, R. J. MacDonald, and W. Rutter. 1979. Isolation of biologically active ribonucleic acid from sources enriched in ribonuclease. *Biochemistry.* 18:5294–5299.

Dahl, G., and W. Berger. 1978. Nexus formation in the myometrium during parturition and induced by estrogen. *Cell Biol. Int. Rep.* 2:381–387.

Daniel, E. E. 1987. Gap junctions in smooth muscle. *In* Cell-to-Cell Communication. W. C. De Mello, editor. Plenum Publishing Corp., New York/London. 149–185.

Darnell, J. E., Jr. 1982. Variety in the level of gene control in eukaryotic cells. *Nature (Lond.).* 297:365–371.

Dupont, E., El Aoumari, A., Roustiau-Severe, J. P. Briand, and D. Gros. 1988. Immunological characterization of rat cardiac gap junctions: presence of common antigenic determinants in heart of other vertebrate species and in various organs. *J. Membr. Biol.* 104:119–128.

Evans, R. M. 1988. The steroid and thyroid hormone receptor superfamily. *Science (Wash. DC).* 240:889–895.

Garfield, R. E., S. M. Sims, and E. E. Daniel. 1977. Gap junctions: their presence and necessity in myometrium during parturition. *Science (Wash. DC).* 198:958–959.

Garfield, R. E., S. M. Sims, M. S. Kannan, and E. E. Daniel. 1978. The possible role of gap junctions in activation of the myometrium during pregnancy. *Am. J. Physiol.* 235:C168–C179.

Garfield, R. E., C. P. Puri, and A. I. Csapo. 1982. Endocrine structural and functional changes in the uterus during premature labor. *Am. J. Obstet. Gynecol.* 142:21–27.

Gilula, N. B., O. R. Reeves, and A. Steinbach. 1972. Metabolic coupling, ionic coupling, and cell contacts. *Nature (Lond.).* 235:262–265.

Gilula, N. B., M. L. Epstein, and W. H. Beers. 1978. Cell-to-cell communication and ovulation. A study of the cumulus-oocyte complex. *J. Cell Biol.* 78: 58–75.

Gimlich, R. L., N. M. Kumar, and N. B. Gilula. 1988. Sequence and developmental expression of mRNA coding for a gap junction protein in Xenopus. *J. Cell Biol.* 107:1065–1073.

Goodenough, D. A., D. L. Paul, and L. A. Jesaitis. 1988. Topological distribution of two connexin32 antigenic sites in intact and split rodent heptocyte gap junctions. *J. Cell Biol.* 107:1817–1824.

Gubler, U., and B. J. Hoffman. 1983. A simple and very efficient method for generating cDNA libraries. *Gene (Amst.).* 25:263–269.

Harley, C. B. 1987. Hybridization of oligo(dT) to RNA on nitrocellulose. *Gene Anal. Tech.* 4:17–22.

Hertzberg, E. L. 1984. A detergent-independent procedure for the isolation of gap junctions. *J. Biol. Chem.* 259:9936–9943.

Hertzberg, E. L., R. M. Disher, A. A. Tiller, Y. Zhou, and R. G. Cook. 1988. Topology of the M_r 27,000 liver gap junction protein. *J. Biol. Chem.* 263: 19105–19111.

Huynh, T. V., R. A. Young, and R. W. Davis. 1984. Constructing and screening cDNA libraries in lambda gt 10 and lambda gt 11. *In* DNA Cloning Techniques: A Practical Approach. D. Glover, editor. IRL Press, Oxford, UK. 49–78.

Ikeda, M., Y. Shibata, and T. Yamamoto. 1987. Rapid formation of myometrial gap junctions during parturition in the unilaterally implanted rat uterus. *Cell Tissue Res.* 248:297–303.

Kistler, J., D. Christie, and S. Bullivant. 1988. Homologies between gap junction proteins in lens, heart, and liver. *Nature (Lond.).* 331:721–723.

Kumar, N. M., and N. B. Gilula. 1986. Cloning and characterization of human and rat liver cDNAs coding for a gap junction protein. *J. Cell Biol.* 103: 767–776.

Laemmli, U. K. 1970. Cleavage of structural proteins during the assembly of the head of bacteriophage T4. *Nature (Lond.).* 227:680–685.

Larsen, W. J., N. H. Tung, and C. Polking. 1981. Response of granulosa cell gap junctions to human chorionic gonadotropin (hCG) at ovulation. *Biol. Reprod.* 25:1119–1134.

Larsen, W. J., S. E. Werft, and G. D. Brunner. 1986. A dramatic loss of cumulus cell gap junctions is correlated with germinal vesicle breakdown in rat oocytes. *Dev. Biol.* 113:517–521.

Loewenstein, W. R. 1981. Junctional intercellular communication: the cell-to-cell membrane channel. *Physiol. Rev.* 61:829–913.

Lowry, O. H., N. J. Rosebrough, A. L. Farr, and R. J. Randall. 1951. Protein measurements with the Folin phenol reagent. *J. Biol. Chem.* 193:265–275.

Manjunath, C. K., and E. Page. 1986. Rat heart gap junctions as disulfide-bonded connexon multimers: their depolymerization and solubilization in deoxycholate. *J. Membr. Biol.* 90:43–57.

Milks, L. C., N. M. Kumar, R. Houghten, N. Unwin, and N. B. Gilula. 1988. Topology of the 32 kd liver gap junction protein determined by site-directed antibody localizations. *EMBO (Eur. Mol. Biol. Organ.) J.* 7:2967–2975.

Nicholson, B., R. Dermietzel, D. Teplow, O. Traub, K. Willecke, and J.-P. Revel. 1987. Two homologous protein components of hepatic gap junctions. *Nature (Lond.).* 329:732–734.

Nicholson, B. J., and J. T. Zhang. 1988. Multiple protein components in a single gap junction: cloning of a second hepatic gap junction protein (MW 21,000). *Mod. Cell Biol.* 7:207–218.

Palmiter, R. D. 1973. Ovalbumin messenger ribonucleic acid translation. *J. Biol. Chem.* 248:2095–2106.

Paul, D. L. 1986. Molecular cloning of cDNA for rat liver gap junction protein. *J. Cell Biol.* 103:123–134.

Puri, C. P., and R. E. Garfield. 1982. Changes in hormone levels and gap junctions in the rat uterus during pregnancy and parturition. *Biol. Reprod.* 27: 967–975.

Saito, Y., H. Sakamoto, N. J. MacLusky, and F. Naftolin. 1985. Gap junctions and myometrial steroid hormone receptors in pregnant and postpartum rats: a possible cellular basis for the progesterone withdrawal hypothesis. *Am. J. Obstet. Gynecol.* 151:805–812.

Tabor, S., and C. C. Richardson. 1987. DNA sequence analysis with a modified bacteriophage T7 DNA polymerase. *Proc. Natl. Acad. Sci. USA.* 84:4767–4771.

Towbin, H., T. Staehelin, and J. Gordon. 1979. Electrophoretic transfer of proteins from polyacrylamide gels to nitrocellulose sheets: procedure and some applications. *Proc. Natl. Acad. Sci. USA.* 76:4350–4354.

Winterhager, E., F. Brümmer, R. Dermietzel, D. F. Hülser, and H.-W. Denker. 1988. Gap junction formation in rabbit uterine epithelium in response to embryo recognition. *Dev. Biol.* 126:203–211.

Yamamoto, K. R. 1985. Steroid receptor regulated transcription of specific genes and gene networks. *Annu. Rev. Genet.* 19:209–252.

Yancey, S. B., S. John, R. Lal, B. Austin, and J.-P. Revel. 1989. The 43-kD polypeptide of heart gap junctions: immunolocalization (I), topology (II), and functional domains (III). *J. Cell Biol.* 108:2241–2254.

Zimmer, P. B., C. R. Green, H. W. Evans, and N. B. Gilula. 1987. Topological analysis of the major protein in isolated intact rat liver gap junctions and gap junction-derived single membrane structures. *J. Biol. Chem.* 262:7751–7763.